

Technique to Collimate Ions in a Hall-Effect Thruster Discharge Chamber

Kunning G. Xu* and Mitchell L. R. Walker†
Georgia Institute of Technology, Atlanta, Georgia 30332

DOI: 10.2514/1.49171

High thrust-to-power ratio on Hall-effect thrusters allows for more efficient thrust generation and better overall performance. It allows Hall-effect thrusters to perform more thrust-intensive maneuvers such as orbit raising, thus saving the mass of a second engine purely for those maneuvers. This paper presents the initial performance measurements of a Hall-effect thruster using in-channel electrodes to collimate ions in the discharge channel in order to increase thrust-to-power. The thruster is tested in the range of 100–300 V discharge voltage, at 9 and 20 A discharge current, and with 0–30 V electrode potential on krypton propellant. Xenon propellant is used briefly. A null-type, inverted pendulum thrust stand is used to acquire thrust measurements. Improvements of 3 mN/kW, 200 s specific impulse, and 4% anode efficiency are observed with energized electrode, supporting the ion collimation hypothesis. Improvements exist primarily at low voltages (<200 V), which indicates a behavior different from the two-stage Hall-effect thruster. Extending the inner channel wall causes a tilt of the magnetic field and severely decreases performance. Plume and in-channel measurements to determine ion collimation are forthcoming.

I. Introduction

HALL-EFFECT thrusters (HETs) are prime candidates for use as primary propulsion systems for satellites. They provide a combination of medium thrust levels and high specific impulse (I_{sp}) that offers weight savings for many near Earth missions. They have been used on many Russian satellites and by the United States on the Loral Space and Communications mobile broadcasting satellite in 2004 and five more in 2009 [1]. Current space mission requirements for propulsion demand a higher thrust-to-power ratio (T/P) for shorter burn times and quicker orbit changes. System studies show using HETs for geosynchronous orbit transfers allow for major mass savings on satellites [2]. Furthermore, a high T/P ratio allows for significant reduction in insertion times. To achieve high T/P ratio operation, the HET must operate at low discharge voltage and high discharge current. In an efficient HET, an increase in the discharge current increases the ion number density as well as the number of ions neutralized by collisions with the discharge channel wall, which decreases efficiency. Thus, increased efficiency at high T/P ratios requires a reduction in ion-wall collisions. The goal of this research is to reduce such collisions through the use of electrodes in the discharge chamber to repel ions away from the wall and focus them toward centerline. The electrodes repel ions with trajectories that intersect the chamber wall, which results in a more collimated ion exhaust plume and increases the efficiency and T/P ratio.

Current state of the art HETs such as the NASA-173M, BHT-1000, BPT-4000, and the H6 generate high T/P ratios at low voltages [3–6]. To date, the BHT-1000 has achieved 96 mN/kW at the 100 V, 2.5 A operating condition [6]. These demonstrate that optimizing the in-channel magnetic field topology will increase performance. In addition to optimizing the magnetic field of the HET, several research efforts have aimed to improve the performance with use of active electrodes in the discharge channel. Previous work with in-channel electrodes or similar additions has focused primarily on creating a

secondary anode for either two-stage operation or control of the anode temperature. Research efforts in both Russia and the United States on the D-80 [7] and D-100 [8] used an emissive electrode between the anode and exit plane for two-stage operation. Raitses used unshielded electrodes of various materials along the inner and outer channel walls to localize and control the acceleration field [9,10]. Kieckhafer studied control of the anode temperature with unshielded in-channel electrodes. The unshielded in-channel electrodes act as a second anode to pull discharge current away from the main anode and thus control Ohmic heating [11]. In both works, the electrodes have various effects on the performance, the most noticeable is a reduction in plume divergence angle [10,11]. The plume divergence reduction effect is mainly attributed to the difference in secondary electron emission coefficient between the metals and ceramics, which results in different sheath and potential drops. The modified wall sheath potential reduces the off-axis velocity component of the ions, which correlates to an increase in thrust. Furthermore, both Raitses and Kieckhafer observed small increases in the T/P ratio. Drawing from their research, it may be possible to enhance the ability of the wall sheath and potential drop to collimate the ion beam through active control of the wall potential.

In this work, in-channel electrodes are added to the Pratt and Whitney Rocketdyne T-220HT to actively control the wall potential at certain locations and thus collimate the ion beam, in order to increase the T/P ratio. This paper details the design and initial performance measurements of the modified T-220HT with a patented in-channel electrode concept. Section II presents the theory and design of the ion focusing electric field and magnetic field within the discharge channel. Section III describes the thruster, facilities, and thrust stand. Section IV presents the results and Sec. V discusses the results and implications.

II. Ion Repulsion and Magnetic Field Design

To increase the T/P ratio at constant power, the mass flow rate and hence discharge current increases as the discharge voltage decreases. Thus, more ions are produced and a larger number of ions are created with large off-axis velocities that eventually impact the discharge channel before exiting the thruster to generate thrust. A reduction in the number of ions that impact the discharge channel wall will further increase the thrust density and T/P ratio of the HET if all other parameters remain constant. The proposed solution to collimate ions is to incorporate positively-biased electrodes along a portion of the discharge channel wall, near the ionization region. The resultant electric field generated by the electrodes will repel ions from the

Received 1 February 2010; revision received 15 June 2010; accepted for publication 9 July 2010. Copyright © 2010 by Kunning G. Xu. Published by the American Institute of Aeronautics and Astronautics, Inc., with permission. Copies of this paper may be made for personal or internal use, on condition that the copier pay the \$10.00 per-copy fee to the Copyright Clearance Center, Inc., 222 Rosewood Drive, Danvers, MA 01923; include the code 0748-4658/11 and \$10.00 in correspondence with the CCC.

*Graduate Research Assistant, High-Power Electric Propulsion Laboratory, Student Member AIAA.

†Assistant Professor, High-Power Electric Propulsion Laboratory, Senior Member AIAA.

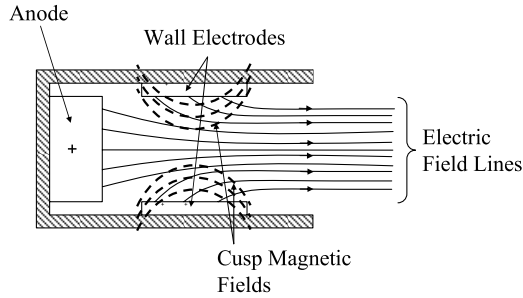


Fig. 1 Electric field with electrodes (notional sketch).

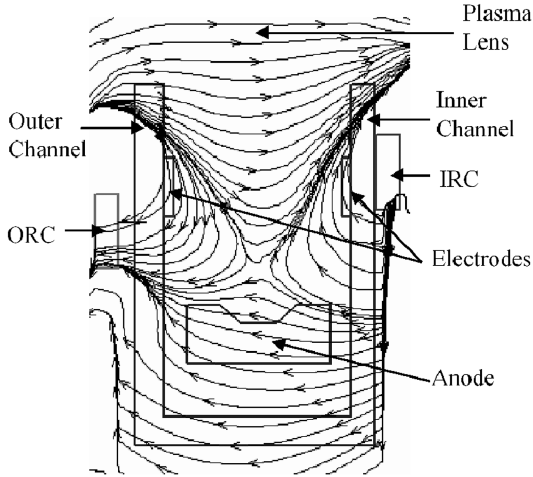


Fig. 2 Simulated magnetic field for the redesigned thruster.

walls and focus their velocity vectors parallel to the thruster axis, which should increase the T/P ratio. Cusp magnetic fields encapsulate the positively-biased electrodes to reduce electron collection, which should prevent a negative impact on efficiency [12]. Figure 1 shows a notional sketch of this concept.

For the electrodes to perform the repulsion function requires their electric field to reach into the channel and affect ions. The distance an electric field penetrates a plasma is determined by the thickness of the plasma sheath. Using average values of electron number density and electron temperature, $2 \times 10^{17} \text{ m}^{-3}$ and 25 eV, respectively, measured 2.5 mm from the wall of the P5 Hall thruster [13], the resultant Debye length is $83 \mu\text{m}$. The plasma sheath can be approximated to be several times the Debye length, which results in a sheath on the order of $<1 \text{ mm}$ in this case [14]. This is a very small fraction of the channel width, and if the electrodes are Debye shielded, they will have little to no effect on the ion trajectories. Previous research shows the ability of magnetic fields to increase sheath thickness when they are parallel or slightly oblique to the surface [15,16]. To increase the effectiveness of the electrodes, cusp-shaped magnetic fields are added surrounding the electrodes.

To generate the ring-cusp magnetic fields, additional electromagnets are added, and the magnetic field topology is redesigned. The effect of the magnetic field topology within the discharge channel has been studied extensively [5,17,18]. The results of past research into this area have concluded that a symmetric, flat, concave plasma lens, as can be seen in Fig. 2, with a low radial magnetic field at the anode results in higher thrust. In addition to magnetic lens

design, this design also incorporates magnetic shielding. Thus the requirements for the magnetic field are: symmetric and flat plasma lens, weak radial field at the anode, and strong cusp fields. All of these requirements were taken into consideration when redesigning the magnetic field of the T-220HT. The commercial software MagNet by Infolytica, a static three-dimensional magnetic modeling code, is used to visualize the fields within the discharge channel.

Figure 2 shows the redesigned magnetic field as well as the locations of the added inner ring-cusp coil, outer ring-cusp coil, and the electrodes. The new field has a flat lens near the exit plane, is predominately symmetric till the anode, and provides ring-cusp magnetic field shielding of the electrodes. The radial field does change direction just downstream of the anode, and forms the beginning of a magnetic mirror. However, the radial strength at the anode is $\sim -20 \text{ G}$ at the highest current levels through the magnets, which will only affect the lowest energy electrons. From measurements provided by Pratt and Whitney of the original magnetic field, the original radial field at the anode is $\sim -10 \text{ G}$ at the same current levels, very close to the modified field. Physical measurements of the centerline radial magnetic field with a mounted Gauss probe match the simulated centerline radial profile except at the anode and exit. The simulated anode radial field is 11 G (30%) smaller than the measured and the exit plane radial field is 46 G (24%) larger than measured. The discrepancy can be attributed to errors in sizing measurements when building simulation model, machining tolerances, Gauss probe accuracy, and probe position accuracy.

The strength of the ring-cusp magnetic field around the electrodes varies with distance from the wall. The minimum necessary strength of the ring-cusp magnetic fields is determined by the Larmor radius of the electrons in the crossed electric and magnetic field near the electrodes. Equation (1) shows that the Larmor radius, r , is determined by the particle mass (m), particle velocity perpendicular to the field (v_{\perp}), particle charge (q), and the strength of the magnetic (B) field. The electron velocity is assumed to be purely thermal. A near-wall electron temperature of 25 eV is assumed based upon electron temperature measurements made by Haas [13]:

$$r = \frac{mv_{\perp}}{|q|B} \quad (1)$$

To achieve a 1-mm Larmor radius in this configuration requires a 95 G magnetic field. The magnetic field simulation gives a field of 110 G at a location 5 mm from the electrode, and the field increases in strength as one approaches the wall. The cusp-field is large enough to magnetize the majority of the electrons and thereby shield the electrodes. Note, that high energy electrons will have an electron gyroradius large enough to reach the biased electrodes.

The effectiveness of the electrodes depends on the energy of the ions themselves. The electrodes will only affect ions with radial energies less than or equal to the electrode voltage. Assuming an acceleration voltage of 200 V, and an ion divergence angle of 30 deg off centerline, this would give a max radial energy of 100 V. Any electrode voltage below 100 V would be unable to fully repel these ions. Another preliminary analysis of electrode effectiveness can be done by comparing an ideal, fully collimated plume to an actual plume. Using data from Hofer [5] and Brown [3] for a 5-kW and 6-kW HET, respectively, one can calculate the difference in the thrust between the ideal case and actual data. Ideal collimated thrust, i.e., no plume divergence, is calculated from the exit velocity of ions, Eq. (2), and the kinetic energy equation, Eq. (3) where T is thrust, \dot{m} is mass flow, v_e is exit velocity, m is mass of a xenon atom, q is charge of an electron, V_a is the acceleration voltage, and λ is the plume divergence

Table 1 Thrust loss due to ion divergence

Thruster	Discharge voltage, V	Discharge current, A	Thrust, mN	λ , deg	Thrust, calculated, mN	Thrust loss, %
NASA-173Mv2	300	8.9	175	35.75	191.8	8.8
H6	300.3	8.81	188.5	-	205.8	8.2
H6	120	9.9	99	39.6	125.3	21
H6	106.2	10.2	91.9	37.5	117.9	22

angle. Table 1 presents the data comparing a few data points for the NASA-173Mv2 and the H6 HET at the University of Michigan:

$$T = \dot{m}v_e \quad (2)$$

$$v_e = \sqrt{\frac{2E}{m}} = \sqrt{\frac{2qV_a}{m}} \quad (3)$$

As the data shows, at 300 V the percent of thrust loss is less than 9%, while at low voltages it is more than 20%. While there are multiple factors that attribute to thrust loss from the ideal case, ion divergence and large radial energies are a significant portion. This brief analysis provides an expected range of thrust improvements that the electrodes in this study could generate. Furthermore, at low voltages the electrodes will increase the thrust more than at high voltages purely because there is a larger thrust loss due to divergence at low voltages.

III. Experimental Setup

A. Hall Thruster

All experiments are performed on a modified Pratt and Whitney Rocketdyne T-220HT HET. Extensive testing has mapped the performance of the thruster over a power range of 2–22 kW at discharge voltages of 200–600 V [19]. The T-220HT has a mean channel diameter of 188 mm, channel depth of 65 mm, and nominal power rating of 10 kW. An Electric Propulsion Laboratory 500 series cathode is located at the three o'clock position of the thruster and parallel to the local magnetic field lines. The cathode orifice is located approximately 30 mm downstream from the front face of the thruster and 178 mm from thruster centerline. The cathode flow rate is set to 1 mg/s for all 9 A cases and 2 mg/s for all 20 A cases investigated. The discharge channel of the thruster is made of M26 grade boron nitride. A more detailed description of the T-220HT and its characteristics can be found in [19].

In the redesign of the magnetic field discussed in section II, a new center magnetic pole was fabricated. The new center pole extends past the lip of the discharge channel, and is exposed to the discharge plasma. A pair of boron nitride (BN) caps is made to cover the pole as shown schematically in Fig. 3. The first cap is a small cap with a smaller diameter than the discharge channel inner wall and shielded only the center pole, leaving a gap between the cap and inner channel where plasma could enter the thruster. Later a second larger cap was made with a diameter equal to the channel inner wall to fully protect the pole and internal components, it, however, also effectively extends the inner channel wall which could interfere with normal operation.

The T-220HT anode is powered by an EMHP 60 kW power supply and all electrical connections enter the chamber through separate feedthroughs. The thruster discharge supply is connected to a filter consisting of a 1.3 Ω resistance and 95 μ F capacitor. The filter acts as a low pass filter preventing oscillations in the current over 1.4 kHz from reaching the discharge supply. High purity (99.999%) krypton and xenon propellant are supplied to the thruster via stainless-steel lines. MKS 1179 A mass flow controllers meter the propellant flow to the cathode and anode. The flow controllers are calibrated by a

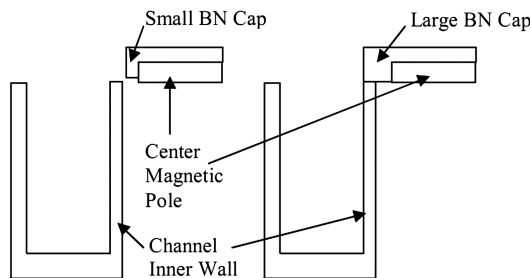


Fig. 3 Small (left) and large (right) BN cap.

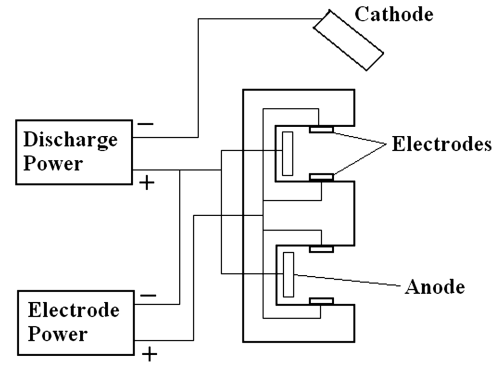


Fig. 4 T-220HT electrode electrical schematic.

custom fixed-volume apparatus by measuring gas pressure and temperature as a function of time.

B. Electrodes

Two set of electrodes are used in the work detailed here, both are stainless-steel bands 0.4 in. (10.16 mm) wide and run the circumference of the inner and outer channels. The first set is 0.015 in. (0.38 mm) thick and the second set 0.05 in. (1.27 mm) thick. The thick electrode was created after the thinner ones melted due to too much current. The electrodes are placed opposite each other 0.715 in. (1.82 cm) upstream of the radial magnetic field peak. They are placed upstream of the ionization/acceleration region to avoid any unexpected interactions such as shorting the Hall current by collecting excess electrons. Upstream of the peak, the electrodes will also be able to affect less energetic ions. The electrodes are electrically connected via welded threaded rods that feed through the rear of the discharge channel. Ceramic sleeves cover the length of the rods to provide electric isolation from the anode and prevent electron absorption. The electrodes are biased above the anode potential during testing. Figure 4 shows the electrode electrical schematic. In this study, both electrodes are connected to the same power supply and are thus biased to the same potential.

C. Thrust Stand

Thrust is measured with a null-type inverted pendulum thrust stand based on the NASA Glenn Research Center design by Haag. The null-type stand holds the thruster at a constant position with use of PID controlled solenoid coils moving a center magnetic rod. Thrust is correlated to the amount of current on the null-coil required to hold the thrust stand at the zero position. Thrust stand calibration is performed by loading and off-loading a set of known weights. The resultant linear curve fit of the null-coil current versus weight (thrust) is used as the conversion for thrust measurements. A water-cooled copper shroud surrounds the stand and is used to maintain thermal equilibrium at 20C. The thrust stand has an average error of $\pm 0.6\%$ of full scale. Further details of the thrust stand and its operation can be found in [20].

D. Measurement Error

The calculated data shown in this paper are composed of T/P , I_{sp} , and anode efficiency. The measured quantities are thrust, discharge voltage, discharge current, and anode mass flow. The thrust stand data has an uncertainty of ± 1.4 mN, the mass flow, voltage, and current measurements all have uncertainties of $\pm 0.1\%$. Error propagation analysis was used to estimate the error in calculated terms. This yields an error of: $T/P \pm 3.5\%$, $I_{sp} \pm 3.6\%$, and efficiency $\pm 5\%$. The accuracy of the electrode current measurement is ± 100 mA.

E. Vacuum Facility

All experiments are performed in the vacuum test facility (VTF) at the Georgia Institute of Technology High-Power Electric Propulsion Laboratory as shown in Fig. 5 below. The VTF is a stainless-steel

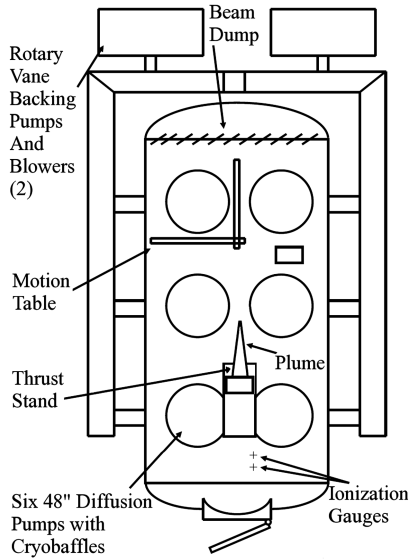


Fig. 5 Schematic of the VTF.

chamber with a diameter of 4 m and length of 7 m. Twin 3800 cubic feet per minute (CFM) blowers and 495 CFM rotary-vane pumps rough the chamber and provide backing for six 48 in. diffusion pumps. The combined nominal pumping speed is 600,000 1/s on air and 155,000 1/s on xenon. The nominal base pressure is in the range of 9×10^{-6} Torr and the operating pressures for this work is below 3.2×10^{-5} Torr, both corrected for krypton and xenon.

IV. Results

The performance of the thruster was measured over a discharge voltage range of 100–300 V at discharge currents of 9 and 20 A on both krypton and xenon propellant. Krypton propellant is used to allow comparison of ion repulsion between krypton and xenon and the effect of ion mass. Krypton has a higher ionization cost compared with xenon, 14 vs 12.1 eV. This causes krypton to have lower energy ions on average because a larger fraction of the available energy is needed for ionization. Xenon is a heavier species, and has higher performance than krypton, in thrust and I_{sp} . Krypton is used for the majority of the testing due to its lower cost. The effect of ion focusing is first investigated at 9 A to determine the durability of the electrodes. A discharge current of 20 A results in a current density of 0.105 A/cm², which results in high HET T/P ratio based on published data. A higher current should result in greater performance improvements with biased electrodes due to the increased number of ions. With more ions, a larger number of them will have large radial velocities that can be focused toward the centerline.

Two center ceramic caps that cover the center pole of the thruster are used. The first is a small cap whose diameter is smaller than the inner channel diameter, and thus should have little to no interaction with the plume. The second is a larger cap whose diameter is equal to the inner channel diameter. The large cap tests the effect of an extended channel wall. Two pairs of electrodes are also used, a thin version with 0.015 in. (0.381 mm) thickness, and a thick version with 0.05 in. (1.27 mm). The experiment seeks to investigate four areas: 1) electrode effectiveness in ion collimation; 2) electrode thickness; 3) influence of an extended channel wall; and 4) impact of ion mass and ionization energy. The results are given in terms of combinations of cap size and electrode thickness.

A. Small Cap, Thin Electrode

The performance of the thruster is measured over a discharge voltage range of 125–250 V at a discharge current of 9 A with krypton and 0.015 in. thick electrodes. The thruster does not operate stably at a discharge voltage of 100 V on krypton and thus this operating condition is not included. The mass flow is held constant for all voltage settings. Test data at 20 A is not available as the thin

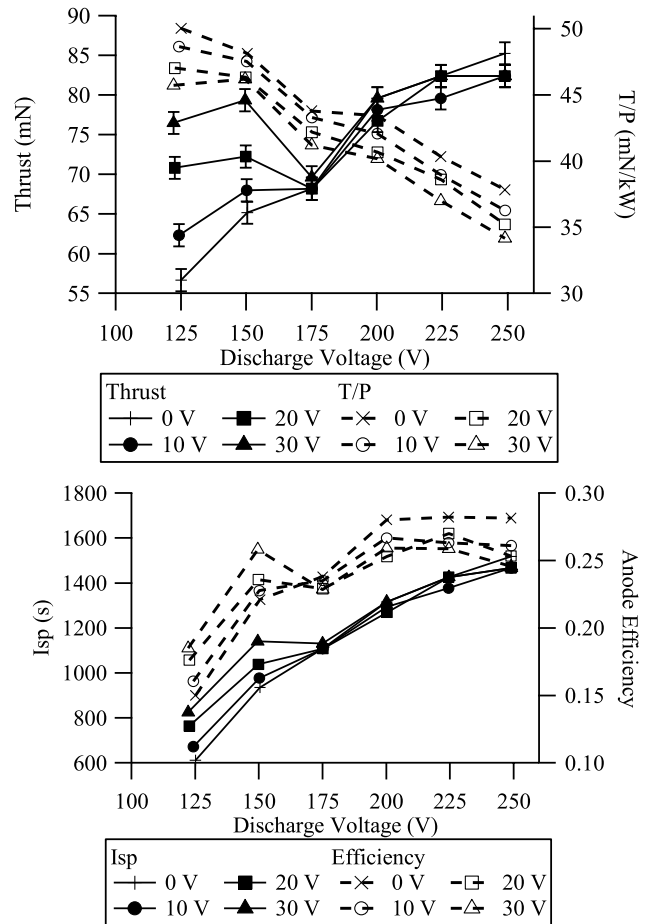


Fig. 6 Small cap, thin electrode performance at 9 A on krypton.

electrodes collected too much current and subsequently had spots of severe melting, severely reducing its operational lifetime. The setup allows the discharge current to change freely when changing electrode voltage. This generally results in an increase in discharge current with electrode voltage. Figure 6 shows the measured thrust, T/P ratio including electrode power, I_{sp} , and anode efficiency of the thruster in this configuration. The calculations of T/P ratio and anode efficiency include the additional power required for the electrodes. For clarity, error bars for T/P ratio, I_{sp} , and anode efficiency are omitted from the figures.

Figure 6 shows an increase in thrust as the electrode voltage increases. The increase is larger at lower discharge voltages. The T/P ratio, however, shows a continual decrease with applied electrode power. The increase in thrust is offset by the additional electrode power, and results in lower T/P ratio than in the case without electrodes. If electrode power is not considered, the T/P ratio increases with applied electrodes. The I_{sp} and anode efficiency both show increases at low voltages and decreases or no change at higher voltages. The switch over point from improvement to no improvement with respect to I_{sp} and efficiency is around 175 V discharge.

B. Small Cap, Thick Electrode

After the thin electrode suffered significant damage due to high Ohmic heating when running at 20 A discharge current, a new thicker set was fabricated and tested. The new 0.05 in. (1.27 mm) thick electrodes are incorporated to withstand the thermal load generated by biasing the electrodes. The thruster is again tested at 9 A over the same range as the thin electrodes, and at 20 A from 125–225 V discharge and 10 V electrode bias. Figure 7 shows the results for the 9 A case. There is a similar increase in thrust at low voltages, but the overall effect is different. Instead of being only effective below 175 V, the electrodes continue to increase thrust up to 225 V. The T/P ratio is also higher with the thick electrodes than thin. The majority of the

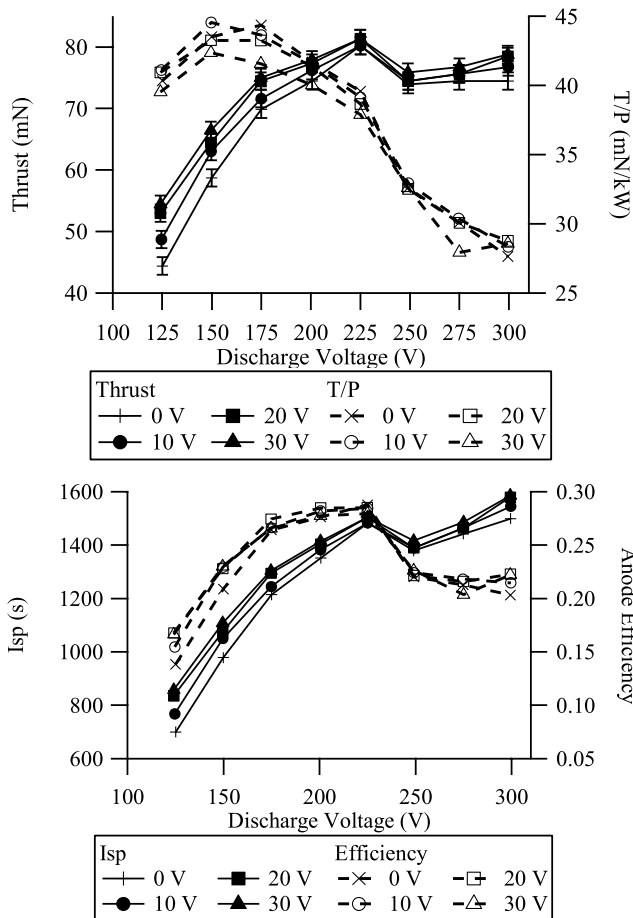


Fig. 7 Small cap, thick electrode performance at 9 A on krypton.

points still show a decrease in T/P ratio with electrode voltage, however, a few points at 125 and 150 V show an increase. The I_{sp} and efficiency also increase as the electrode voltage increases, but the increase is not as large compared with the thin electrodes. At 125 V, the small/thin configuration shows a 213 s in I_{sp} and a 3.5% increase anode efficiency, whereas the small/thick configuration only shows an increase of 157 s in I_{sp} and 2.8% in anode efficiency. The increases in thrust, I_{sp} , and efficiency persists until 225 V with thick electrodes as opposed to 175 V with the thin electrodes.

Figure 8 shows the small/thick configuration at a discharge current of 20 A. The thrust, T/P ratio, I_{sp} , and efficiency improvement with electrode is higher for 20 than 9 A. This seems to confirm the idea that biased electrodes generate larger performance improvements at higher discharge currents. The larger number of ions generated at high currents means more ions are repelled from the wall and focused toward centerline, thus generating more thrust.

C. Large Cap, Thick Electrode

The final configuration tested is the thick electrodes with the large cap that has the same diameter as the inner channel wall. The cap thus effectively lengthens the inner channel wall. Changing the channel length can have improve thruster performance by improving propellant utilization and efficiency [21]. Test points are run at nine on both krypton and xenon propellant. Figure 9 shows the performance at 9 A on krypton. The thrust improvement is smaller in magnitude compared with the tests with the small cap. This causes a greater decrease in the T/P ratio with electrodes. The I_{sp} also has a smaller improvement compared with previous configurations. The cause of this change can be attributed to two changes, the use of the large cap, and a changed optimal magnetic field which will be discussed in the next section.

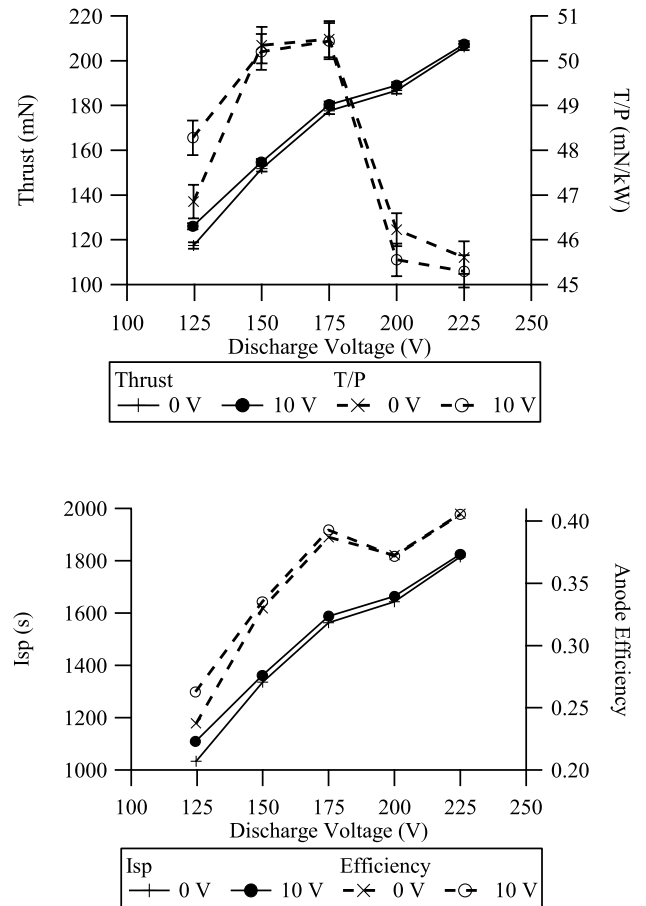


Fig. 8 Small cap, thick electrode performance at 20 A on krypton.

Figure 10 shows the data taken with the large cap and thick electrode at 9 A on xenon. The xenon no electrode performance is higher than krypton in all four metrics. The increases in thrust, I_{sp} and efficiency with electrodes are lower for xenon than krypton, however.

V. Discussion

A. Electrode Effects

In all of the data sets, there is a consistent increase in thrust, I_{sp} , and anode efficiency at low voltages. The increase in thrust at low voltages indicates that the electrodes enhance the ability of the thruster to create a collimated ion plume. Whether this is through ion focusing or some other effect, such as a two-stage operation, cannot be determined from the performance data alone. However, the fact the improvements only exist at low voltages, runs contrary to previous work on two-stage HETs, which indicates improvements primarily at high voltages [17,22]. This suggests that the electrodes do not function as a second stage. Raitses work with unshielded electrodes shows little to no performance improvement in the voltage range of 170 to 300 V, which again suggests that the changes seen here are not the result of two-stage operation [23].

The calculated plasma sheath around the electrodes is on the order of <1 mm. This would mean the electrodes can only affect a small portion of ions, and should have little effect on thruster performance metrics such as thrust. Yet, noticeable changes in thrust are measured. The presence of the ring-cusp magnetic fields that shield the electrodes complicates the plasma sheath analysis. The ring-cusp magnetic fields greatly retard the motion of electrons that move perpendicular to the magnetic field, which prevents a thin electron sheath from forming around the electrode and extends the distance the electric field penetrates into the plasma. Ions are depleted in the sheath due to the electric field from the electrodes and are too heavy to be affected by the ring-cusp fields. Therefore, the calculated value of <1 mm sheath thickness is likely incorrect. Anders et al. [15] and

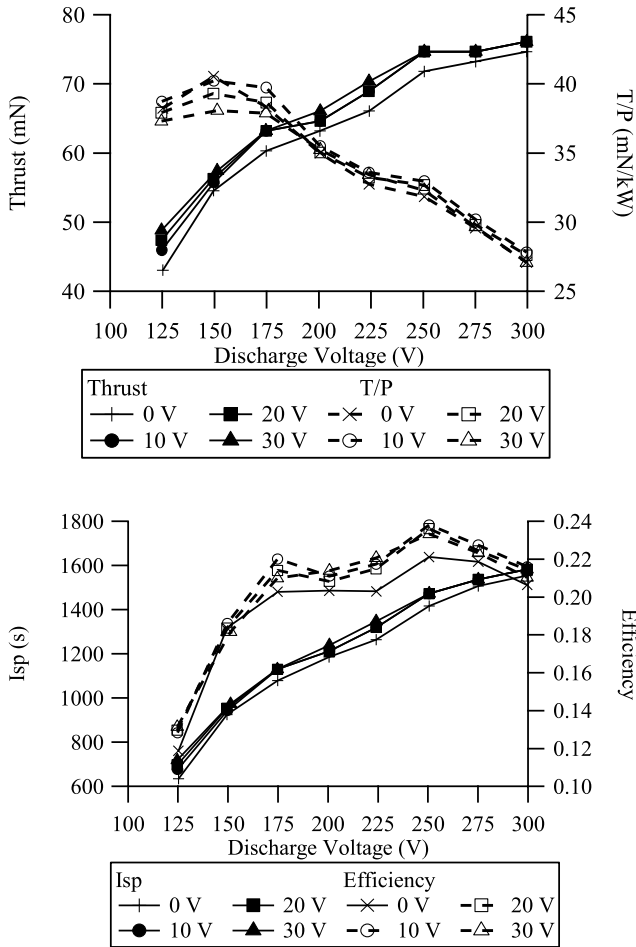


Fig. 9 Large cap, thick electrode performance at 9 A on krypton.

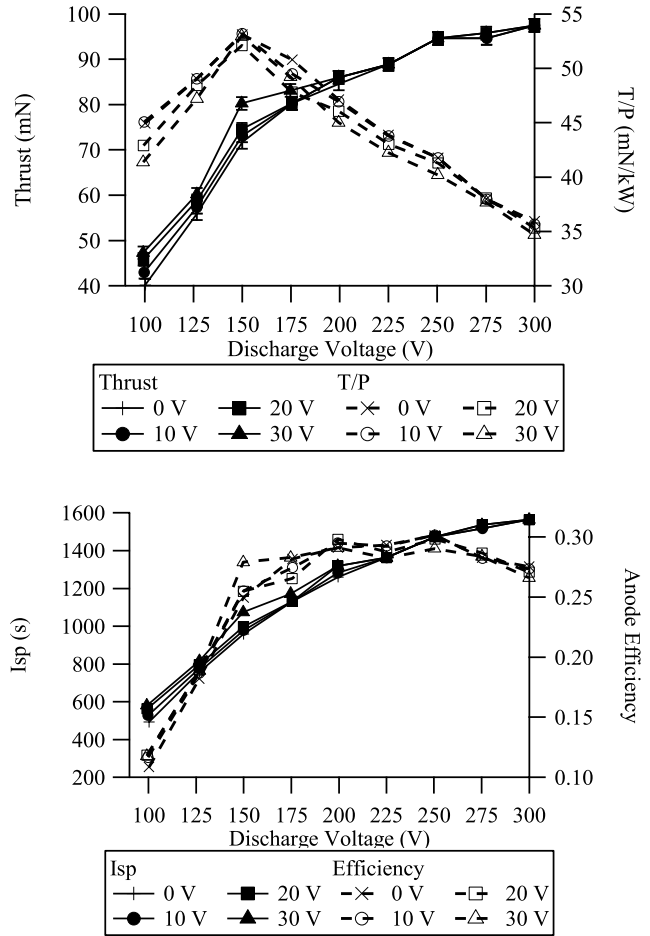


Fig. 10 Large cap, thick electrode performance at 9 A on xenon.

Keidar and Beilis [24] show that a parallel magnetic field along a positively-biased wall extends the plasma sheath away from the wall for field strengths measuring at least a few hundred Gauss. The ring-cusp magnetic fields around the electrodes in this study are 100–300 G. Thus, the sheath and the electric field probably extend significantly farther than 0.8 mm into the discharge plasma. How far the field penetrates is not known at this time and a subject of interest and future investigation.

Assume for a moment the electrodes are able to affect the entire width of the channel, it will then change the local electric field and the overall potential profile. Fruchtman modeled a similar setup of an HET with in-channel electrodes and showed that the addition of a biased electrode can cause a sonic transition and an increase in thruster efficiency [25]. That work differs in that his electrode was biased slightly below anode potential, to create a two step potential profile. Electrons in the anode-electrode region would have slower velocities, thus increasing number density and ionization. In this work, since the electrodes are at a higher potential than the anode, the potential profile has a peaked shape. The electric potential is highest at the electrode location and decreases toward both cathode and anode. Electrons moving toward the anode will be accelerated by the potential between cathode and electrode, but then slowed by the lower potential anode. This can increase the electron number density in the region between anode and electrode, thus increasing ionization in that region in the same manner as Fruchtman.

For ions, however, any created between the anode and electrode region would preferentially move toward the anode due to its lower potential. This suggests that ions created in this region may be neutralized by the anode and result in a loss factor. This likely a small effect, since the electrodes do produce higher thrust. The behavior of the charged particles to the peaked profile will be examined in the future.

A phenomenon common to all the data sets is that the beneficial effects of the electrode decreases as discharge voltage increases. This is reasonable, because at high voltages a smaller fraction of the energy is needed for ionization, thus more is available for acceleration compared with low voltages where there is much less energy for acceleration [26]. This results in lower energy ions at low voltages and higher energy ions at high voltages relative to the discharge voltage. From the simple analysis presented in the beginning of this study, at high voltages the electrodes at 30 V will not fully repel and turn ions with a 100 V radial energy perpendicular to the wall. In contrast, for a low voltage operation, acceleration voltage of 90 V, with the same divergence angle of 30 deg, the maximum radial energy is 45 V. Thus, the 30 V electrodes will repel and turn a much

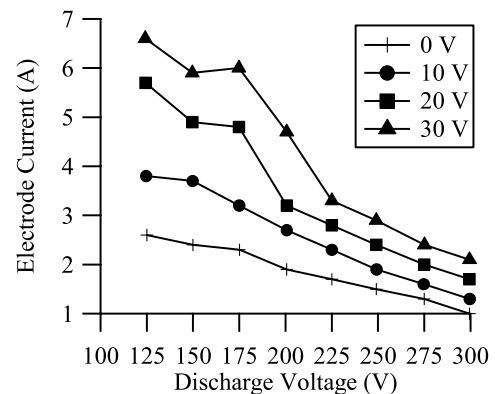


Fig. 11 Electrode current at 9 A on krypton for small cap, thick electrode.

larger portion of the ions at this operating condition. This may be why there is a larger improvement in thrust at low discharge voltages.

A second explanation would be more ions are lost at high voltages due to the peaked potential profile in the channel. As stated previously, ions created in the anode-electrode region may preferentially move toward the lower potential anode and become neutralized. As discharge potential increase, electron energy increases and the electron are better able to ionize atoms. The increased energy, coupled with the increased electron number density in the anode-electrode region could result in the creation of more ions at high voltages than at low. The ion-anode neutralization loss factor may become more significant at higher discharge voltages, thus explaining the decreased performance with electrodes at those voltages.

The electrode current during these tests provides an idea of the electron behavior within the channel relative to the biased electrodes. Figure 11 shows the electrode current for the small cap with thick electrode for a 9 A discharge current on krypton. The electrode current increases as the electrode voltage increases. This is because as the electrode voltage increases, the electron attraction to the electrode is stronger, which results in a higher electrode current despite the same electron trapping field. As discharge voltage increases, the decreasing electrode current suggests either the anode is collecting an increasingly large portion of the electron current, or the ion beam current is a larger fraction of total current. The former is more likely. As the discharge voltage increases, the additional voltage on the electrodes, 10–30 V, becomes a smaller fraction of the anode voltage. For example, 30 V electrodes at 100 V anode voltage results in the electrodes having a 30% higher potential as the electrodes are biased above anode potential, however, if anode potential is 300 V, the same electrode only has a 10% higher potential. The additional potential from the electrodes are thus a small fraction, and electrons are less likely to be attracted to the electrodes.

B. Electrode Thickness Effects

The thick electrodes are more than 3 times the thickness of the thin electrodes. The thick electrodes reduce the channel cross-sectional area by 10%. Figure 12 shows thrust measurements for the thin and thick electrodes. When the thick electrodes are placed into the channel, the performance improvements are smaller than with the thin electrodes. Not only does the thick electrode have overall less thrust, even with 0 V on the electrode, the thrust increases are smaller. The one exception is at 175 V where the thin electrodes seemed to have no effect. One simple theory for the change in performance is that the thicker electrodes are a larger obstacle than the thin electrodes, which cause more ions to impact the electrode. The thick electrodes did generate T/P ratio increases where the thin electrode did not even though the thin set generated higher thrust. This is due to increased electron absorption by the thin electrodes; however why the thin set absorbs more current is unknown at this time.

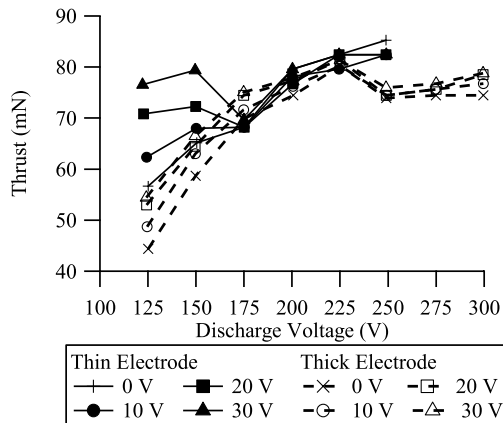


Fig. 12 Thrust for thin and thick electrodes.

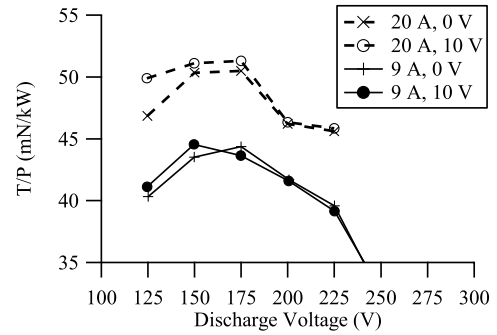


Fig. 13 Thrust-to-power ratio for 9 and 20 A discharge current on krypton.

Figure 13 combines the T/P ratio data from the 9 and 20 A tests using the thick electrode to allow direct comparison of the differences in performance improvements at the two current levels. The T/P ratio for the 20 A tests is better than the 9 A tests. The improvements also span a wider range of voltages. This gives support to the idea the electrodes perform better at high currents because of a higher ion density.

C. Extended Channel Wall

To test how well the electrodes collimate the plume, a large cap that extends the inner channel wall is added. With the large cap, there was a large drop in the performance gains, 2–10% decrease in thrust improvement depending on the conditions. The likely sources for this change are a changed magnetic field and the interfering presence of the larger cap. The T-220HT thruster is designed with a symmetric field with flat plasma lens, as shown in Fig. 2, generated by the magnets energized with equal amounts of current, this minimizes the discharge current. The added ring-cusp magnet coils affect the discharge current minimally, but help reduce the electrode current. This setting of currents gives the lowest discharge current when using the small cap. When the large cap is installed, the currents required to give minimum discharge current changes. Instead of a balanced current setting resulting in a flat plasma lens, the thruster dictated an outward tilted plasma lens to give minimal discharge current. A simulation of the resultant magnet field with these setting is shown in Fig. 14. As the simulation shows, the magnetic field is pushed outward, away from the inner wall. The outer electrode becomes completely unshielded. The plasma lens is also pulled upstream of the exit plane and tilted toward the outer channel (left). All these field changes would contribute a great deal to the performance degradation. The tilted plasma lens focuses the plume outward, farther away from centerline, which increases the radial portion of the ion velocity, and thereby decreases thrust.

This type of behavior points to the plasma wanting to stay away from the inner wall. Indeed, it has been visually noticed that the inner

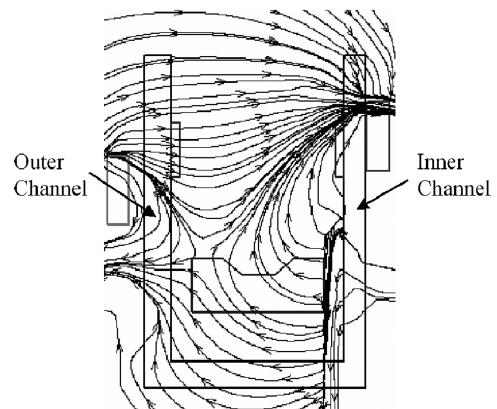


Fig. 14 Tilted magnetic field.

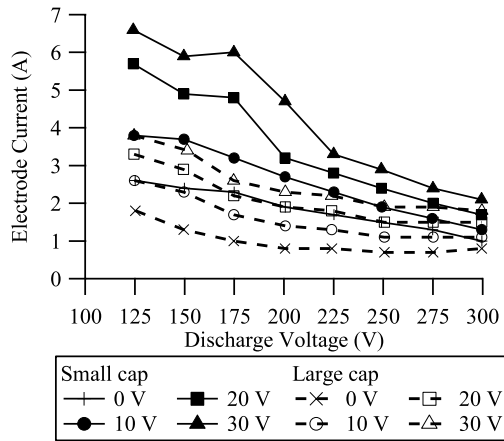


Fig. 15 Electrode current for small cap and large cap with extended wall at 9 A on krypton.

electrode see high Ohmic heating before the outer electrode, suggesting the inner electrode is responsible for the majority of the electrode current. This is seen clearly in Fig. 15 where electrode current for small cap and large cap data with the thick electrodes at 9 A are shown. The large cap with the extended wall has both a lower average current level and a slower increase as discharge voltage decreases. This points to the inner electrode absorbing a large portion of the electrode current.

The effect of the outward tilted magnet field could be to keep the electrons away from the inner electrode. A few test points not shown here were run at a balanced magnet current setting. Both the discharge and electrode current increased compared with the previous tests, and the outer edge of the large cap becomes red hot. The glowing of the cap suggests that large numbers of ion impact the large cap. This means the electrodes do not collimate the ion beam as much as is desired. The large cap is likely located in or just past the acceleration region, and any ions moving toward the thruster centerline with large enough angle are impacting the cap. Ion impacts with the wall due to radial ion velocities cause decreased performance with the extended inner wall.

D. Krypton vs Xenon

The baseline performance of the thruster on xenon is higher than that with krypton. Xenon propellant is expected to have larger performance increases with the applied electrode because the ionization energy of xenon is lower than that of krypton, which results in a larger number of xenon ions for the same energy. The data shows roughly the same percentage increase in performance with electrodes over no electrodes for krypton and xenon. On xenon, as the discharge voltage increases, the performance gains disappear and instead the electrodes decrease T/P ratio, I_{sp} , and efficiency. Why the use of xenon resulted in such a large drop in performance with in-channel electrodes is not known at this time. A guess can be made in the vein of the peaked potential profile. Xenon's lower ionization energy compared with krypton would result in more ions formed in the anode-electrode region, thus increasing the significance of the neutralization loss.

VI. Future Work

Future research will involve plasma measurements to determine the behavior of ions in response to the electrodes and cusp-shaped magnetic fields. The diagnostics to be used are a Faraday probe and a retarding potential analyzer to measure ion current density and ion energies, respectively, at locations in the plume. The measurements will allow determination of the plume divergence angle, and ion energies at known angles. An increase in the total current density with energized electrodes, obtained by integrating the current density over the plume, would indicate an increase in ion number density and decreased ion-wall neutralizations. Ion energy measurements allow

determination of the ion radial velocity. Knowing the energy and angle from centerline, the portion of the energy in the radial direction can be determined. A decrease in the net plume angle with electrodes while maintaining same ion energies would indicate a decreased ion radial energy. These two measurements will allow determination of the effectiveness of the ion repulsion effect of the electrodes.

VII. Conclusions

A study was conducted to investigate the effect of ion focusing in HETs with in-channel electrodes. A pair of electrodes are laid against the surface of the inner and outer channel walls and biased slightly above anode potential. Different center cap sizes and electrode thicknesses are tested. The results show there is a definite thrust, I_{sp} , and anode efficiency increase when the electrodes are powered and evidence suggests this is due to ion focusing exists. Thrust, I_{sp} , and anode efficiency all increase, especially at lower discharge voltages, with increasing electrode voltage. T/P however shows minimal improvement due to the additional power from the electrodes offsetting any thrust gain. Operating at higher current levels resulted in larger improvements over a wider range of discharge voltages. Xenon propellant produced higher baseline performance as expected, but any improvements generated by the electrodes are equal to or smaller in magnitude than that observed with krypton. The cause for this is not known at this point and will be a goal of future investigations. More work, including plume diagnostic and in-channel plasma measurements, is needed to fully understand the effects the electrodes are having on the thruster. Future papers will present more in-depth investigations into the effectiveness of the electrodes in collimating ions.

Acknowledgments

The research contained herein was sponsored by the U.S. Air Force Research Laboratory (James Haas is the contract monitor) and American Pacific In-Space Propulsion. We would like to thank Pratt and Whitney for supplying High-Power Electric Propulsion Laboratory (HPEPL) with the T-220HT, Gregory McCormick for work in simulation and modifications, and departmental technical staff and other graduate students at HPEPL for assistance with this work. Kunming Xu is supported by the National Defense and Science Engineering Graduate Fellowship. The authors are greatly appreciative of this support.

References

- [1] Rovey, J. L., "2009: The Year in Review," *Aerospace America*, Vol. 47, AIAA, Reston, VA, 2009, p. 44.
- [2] Byers, D. C., and Dankanich, J. W., "Geosynchronous-Earth-Orbit Communication Satellite Deliveries with Integrated Electric Propulsion," *Journal of Propulsion and Power*, Vol. 24, No. 6, 2008, pp. 1369–1375. doi:10.2514/1.35322
- [3] Brown, D. L., "Investigation of Low Discharge Voltage Hall Thruster Characteristics and Evaluation of Loss Mechanism," Ph.D. Dissertation, Dept. of Aerospace Engineering, Univ. of Michigan, Ann Arbor, MI, 2009.
- [4] de Grys, K., Rayburn, C., Wilson, F., Fisher, J., Werthman, L., and Khayms, V., "Multi-Mode 4.5 kW BPT-4000 Hall Thruster Qualification Status," 39th AIAA Joint Propulsion Conference, AIAA Paper 2003-4554, Huntsville, AL, 2003.
- [5] Hofer, R. R., "Development and Characterization of High-Efficiency, High-Specific Impulse Xenon Hall Thrusters," Ph.D. Dissertation, Dept. of Aerospace Engineering, Univ. of Michigan, Ann Arbor, MI, 2004.
- [6] Pote, B., and Tedrake, R., "Performance of a High Specific Impulse Hall Thruster," 27th International Electric Propulsion Conference, IEPC Paper 01-35, Pasadena, CA, 2001.
- [7] Butler, G. W., Yuen, J. L., Tverdokhlebov, S. O., Semekin, A. V., and Jankovsky, R. S., "Multimode, High Specific Impulse Hall Thruster Technology," 36th AIAA Joint Propulsion Conference, AIAA Paper 2000-3254, Huntsville, AL, 2000.
- [8] Tverdokhlebov, S. O., "Study of Double-Stage Anode Layer Thruster Using Inert Gases," 26th International Electric Propulsion Conference,

- IEPC Paper 93-232, 1993.
- [9] Fisch, N. J., and Raitsev, Y., "Design and Operation of a Hall Thruster with Segmented Electrodes," 35th AIAA Joint Propulsion Conference, AIAA Paper 99-2572, Los Angeles, 1999.
- [10] Raitsev, Y., Dorf, L. A., Litvak, A. A., and Fisch, N. J., "Plume Reduction in Segmented Electrode Hall Thruster," *Journal of Applied Physics*, Vol. 88, No. 3, 2000, pp. 1263–1270. doi:10.1063/1.373813
- [11] Kieckhafer, A. W., "The Effect of Segmented Anodes on the Performance and Plume of a Hall Thruster," Ph.D. Dissertation, Dept. of Mechanical Engineering, Michigan Technological Univ., Houghton, MI, 2007.
- [12] Goebel, D. M., and Katz, I., *Fundamentals of Electric Propulsion: Ion and Hall Thrusters*, Jet Propulsion Lab., Pasadena, CA, 2008.
- [13] Haas, J. M., "Low-Perturbation Interrogation of the Internal and Near-Field Plasma Structure of a Hall Thruster Using a High-Speed Probe Positioning System," Ph.D. Dissertation, Dept. of Aerospace Engineering, Univ. of Michigan, Ann Arbor, MI, 2001.
- [14] Chen, F. F., *Introduction to Plasma Physics and Controlled Fusion, Vol 1, Plasma Physics*, Springer, New York, 2006.
- [15] Anders, A., Anders, S., and Brown, I. G., "Effect of Duct Bias on Transport of Vacuum Arc Plasmas Through Curved Magnetic Filters," *Journal of Applied Physics*, Vol. 75, No. 10, 1994, pp. 4900–4905. doi:10.1063/1.355777
- [16] Beilis, I. I., and Keidar, M., "Sheath and Presheath Structure in the Plasma-Wall Transition Layer in an Oblique Magnetic Field," *Physics of Plasmas*, Vol. 5, No. 5, 1998, pp. 1545–1553. doi:10.1063/1.872813
- [17] Hofer, R. R., Peterson, P. Y., and Gallimore, A. D., "A High Specific Impulse Two-Stage Hall Thruster with Plasma Lens Focusing," 27th International Electric Propulsion Conference, IEPC Paper 01-036, Pasadena, CA, 2001.
- [18] Belikov, M. B., Gorshkov, O. A., Rizakhanov, R. N., and Shagayda, A. A., "Hall-Type Low-and-Mean-Power Thrusters Output Parameters," 35th Joint Propulsion Conference, AIAA Paper 99-2571, Los Angeles, 1999.
- [19] McVey, J. B., Britt, E. J., Engelman, S. F., Gulczinski, F. S., Beiting, E. J., and Pollard, J. E., "Characteristics of the T-220HT Hall-Effect Thruster," 39th Joint Propulsion Conference, AIAA Paper 2003-5158, Huntsville, AL, 2003.
- [20] Xu, K. G., and Walker, M. L. R., "High-Power, Null-Type, Inverted Pendulum Thrust Stand," *Review of Scientific Instruments*, Vol. 80, No. 055103, 2009. doi:10.1063/1.3125626
- [21] Raitsev, Y., Ashkenazy, J., and Guelman, M., "Propellant Utilization in Hall Thrusters," *Journal of Propulsion and Power*, Vol. 14, No. 2, 1998, pp. 247–253. doi:10.2514/2.5274
- [22] Jacobson, D. T., Jankovsky, R. S., and Rawlin, V. K., "High Voltage TAL Performance," 37th AIAA Joint Propulsion Conference, AIAA Paper 2001-3777, Salt Lake City, UT, 2001.
- [23] Fisch, N. J., Raitsev, Y., Dorf, L. A., and Litvak, A. A., "Variable Operation of Hall Thruster with Multiple Segmented Electrodes," *Journal of Applied Physics*, Vol. 89, No. 4, 2001, pp. 2040–2046. doi:10.1063/1.1337919
- [24] Keidar, M., and Beilis, I. I., "Plasma-Wall Sheath in a Positive Biased Duct of the Vacuum Arc Magnetic Macroparticle Filter," *Applied Physics Letters*, Vol. 73, No. 3, 1998, pp. 306–308. doi:10.1063/1.121817
- [25] Fruchtman, A., Fisch, N. J., and Raitsev, Y., "Control of the Electric-Field Profile in the Hall Thruster," *Physics of Plasmas*, Vol. 8, No. 3, 2001, pp. 1048–1056. doi:10.1063/1.1343508
- [26] Brown, D. L., Larson, W., and Beal, B. E., "Methodology and Historical Perspective of a Hall Thruster Efficiency Analysis," *Journal of Propulsion and Power*, Vol. 25, No. 6, 2009, pp. 1163–1177. doi:10.2514/1.38092

J. Blandino
Associate Editor